A hybrid microfluidic platform for cell-based assays via diffusive and convective trans-membrane perfusion

Elizaveta Vereshchagina,[1] Declan Mc Glade,[1,a] Macdara Glynn,[2] and Jens Ducrée[1,2,b]

[1]*School of Physical Sciences, National Centre for Sensor Research, Dublin City University, Dublin 9, Ireland*
[2]*Biomedical Diagnostics Institute, National Centre for Sensor Research, Dublin City University, Dublin 9, Ireland*

We present a novel 3D hybrid assembly of a polymer microfluidic chip with polycarbonate track-etched membrane (PCTEM) enabling membrane-supported cell culture. Two chip designs have been developed to establish either diffusive or convective reagent delivery using the integrated PCTEM. While it is well suited to a range of cell-based assays, we specifically employ this platform for the screening of a common antitumor chemotoxic agent (mitomycin C – MMC) on the HL60 myeloid leukemia cell line. The toxic activity of MMC is based on the generation of severe DNA damage in the cells. Using either mode of operation, the HL60 cells were cultured on-chip before, during, and after exposure to MMC at concentrations ranging from 0 to 50 μM. Cell viability was analysed off-chip by the trypan blue dye exclusion assay. The results of the on-chip viability assay were found to be consistent with those obtained off-chip and indicated ca. 40% cell survival at MMC concentration of 50 μM. The catalogue of capabilities of the here described cell assay platform comprises of (i) the culturing of cells either under shear-free conditions or under induced through-membrane flows, (ii) the tight time control of the reagent exposure, (iii) the straightforward assembly of devices, (iv) the flexibility on the choice of the membrane, and, prospectively, (v) the amenability for large-scale parallelization. © *2013 AIP Publishing LLC*. [http://dx.doi.org/10.1063/1.4804250]

I. INTRODUCTION

Despite notable advances in the development of biomedical diagnostic devices and a large market of currently established tools, there is a continuously growing demand for miniaturized, low-cost[1] devices that can accurately control *in vivo* conditions for cell culture, handling, and analysis with minimum user intervention. If equipped with a set of key on-chip fluidic operations that are highly configurable and manufactured at low cost,[1] these devices bear great promise in high-throughput, automated drug discovery[2] and screening[3] and also lend themselves for point-of-care settings by relatively unskilled personnel. Ideally, such platforms should assist in monitoring multiple aspects of cell physiology, be compatible to various types of cellular assays, and, yet, provide a large degree of freedom in adjustment of experimental conditions with reduced consumption of reagents and cells. Increasing the functionality of such systems while, at the same time, adopting a standard chip format reduces the time and cost of manufacturing. Furthermore, this strategy opens an opportunity for further system-level integration with bio-diagnostic tools characterised by a higher degree of complexity.

Prior to analysis of cell populations, the cells first need to be temporally isolated or confined to a region that can be investigated on a chip. One of the common approaches for high-

---

[a]Present address: Microbial Ecology Group, School of Biotechnology, Dublin City University, Dublin 9, Ireland.
[b]Author to whom correspondence should be addressed. Electronic mail: jens.ducree@dcu.ie. Tel.: +353 1 700 5377.

throughput cell trapping and sorting in microfluidic cell-based perfusion systems is to geometrically restrict the location of the target cells by introducing a trench,[4–6] microwell,[7] trap,[8] array of geometrical cell restrictors,[9,10] hydrogel-based scaffolds,[11,12] and cell chambers.[13] An alternative, simple, and comparatively rarely explored method is to introduce membrane-integrated devices where an embedded biocompatible and porous membrane physically separates the culture compartment from the flow carrying microfluidic structures.[14] Thus, the device simultaneously provides a means for controlling membrane-mediated drug transport and a support for (long-term) cell culture experiments. Such hybrid integration of commercial, biocompatible membranes with a homogeneous pore distribution already supports uniform cross-membrane flow and a pressure drop across the culture wells, eliminating any further need for complex flow homogenizers or fluid distributing networks.[15]

The membrane-to-chip assembly technology is widely covered in the literature and takes its roots in microsystems for analytical chemistry where membranes in microreactors are used for mixing, gas-liquid contacting, emulsification, filtration, sample purification, concentration or pre-treatment, and adsorptive and other catalytic studies.[16] The majority of these systems are based on silicon technology or *in situ* synthesis of membranes[17] and are used for the fabrication of membranes with very specific properties—not always suitable to cell-based studies. Moreover, in these cases, the manufacturing can be relatively complex, time consuming, and pricy, thus seriously impeding the success of silicon- or glass-based fabrication processes in the very cost-conscious bio-diagnostic arena. 3D polymeric hybrid systems with integrated membranes for cellular assays constitute a relatively new research field demanding new engineering concepts with a high degree of compatibility to established rapid prototyping technologies and bio-samples.

As the membrane-assisted devices arose from traditional, bio-analytical applications over the last decade,[18] a variety of new chip devices for studying cells and biomimetic systems were introduced. Among these are a perfusion system for high resolution microscopy on living cells,[19] chips performing Calcein-AM cell viability assays,[20] assisting in integration of intestinal epithelium,[21] a bioreactor for monitoring kidney epithelial cells,[22] systems for proteomic studies[23] such as the trapping of lectin protein complexes,[24] so-called organ-on-a-chip systems[25] (which mimic, for instance, the physiology of human lung[26] and blood vessels[27]), devices for studies of bacterial chemotaxis[28] and aerotaxis,[29] and systems applied to the study of thrombosis and hemostasis.[30] Additionally, membranes were shown useful as a mask for direct patterning of proteins.[31] The majority of the above mentioned systems are based on cast-moulded Polydimethylsiloxane (PDMS) and are therefore quite limited in fabrication throughput, shelf life, as well as their range of compatible solvents and chemical reagents. Also, these systems were primarily designed to address one particular application, thus lacking a generic concept suitable for a range of different cell-based assays.

Various technological approaches have been demonstrated for direct integration of polymeric membranes, such as gluing,[32] sandwiching,[19] clamping[33] between flexible PDMS or rigid polymeric materials, or direct *in situ* fabrication as a part of a microfluidic device using 3D printing technology.[34] However, such direct incorporation of commercial membranes with commonly used polymeric materials still remains technologically challenging. The main obstacles lie in the sealing step due to the anti-sticking properties of the majority of rapid prototyping polymeric materials and excessive membrane thickness or fragility. As a result, poor sealing may lead to leakages or poor control over device performance. Another particular difficulty is the reproducibility in manufacturing (particularly for the membranes which are only tens of microns in thickness) while meeting the need for a sterile cell culture environment and ensuring consistent flow conditions across the parallelized cell culture chambers during device operation.

In the present paper, we describe the design, fabrication, and operation of a microfluidic platform for cell-based assay studies in various flow regimes. The performance of the system is demonstrated by long-term culturing of HL60 human leukemic cells, whilst controllably exposing the cells to a dilution series of a cytotoxic drug, the cellular exposure of which can be estimated via an off-chip toxicity assay. The platform is based on mass manufacturable poly (methyl methacrylate) (PMMA) chip base and biocompatible, polycarbonate track-etched

membranes (PCTEMs); these constituents are sealed via adhesives. The advantage of the here presented assembly process is its simplicity as well as its amenability to a comprehensive catalogue of application-specific commercial membranes, e.g., featuring specific porosities, thicknesses, and morphologies. Therefore, a variety of applications and bioassay readout schemes, for instance colorimetric or fluorimetric, can be implemented by the choice of the membrane. Two fluidic designs and corresponding modes of operation are investigated in this paper and supported by computational fluid dynamics (CFD) modelling. The suitability of the platform for cell-based assays was demonstrated with a pilot study on the on-chip cultivation of HL60 with a directed and controlled exposure to a chemotoxic drug mitomycin C (MMC).[35] The results of cell viability assays performed on-chip are in good agreement with those obtained from a standard microtiter plate. The actual cell seeding and cultivation took place on-chip and only the detection was off-chip. Alternative types of perfusion systems require that cells be seeded in a microtiter plate and only then transferred to the system for further analysis, which implies a longer and more complex experimental procedure.[15]

The primary potential of the biomimetic system lies in the simplistic integration of any type of bio-compatible transport control system by means of a thin membrane into a rigid microfluidic system made of PMMA, as well as the simple, low-cost, and flexible system fabrication and assembly process. The developed platform demonstrates reproducible performance in both operation regimes and is deemed suitable for a wide range of cellular bioassays.

Throughout the following sections, we discuss the operational principle of the two membrane-based platforms supported by the CFD modelling, the fabrication procedure, and the results of the HL60 cell viability assay carried out using this platform. The paper is intended to provide sufficient background information on design and fabrication aspects of hybrid polymeric membrane-based microfluidic platforms suitable for various cellular studies.

II. WORKING PRINCIPLE AND APPLICATION

The 3D schematic featuring the basic working principle of the two implemented microfluidic platforms—flow-through and diffusion-based—is illustrated in Figure 1. Each chip is composed of a top sealing layer containing the aeration holes (Fig. 1(a)), a bottom fluidic part integrating the cell-culture wells, the fluidic supply channels, and the interspersed membrane in
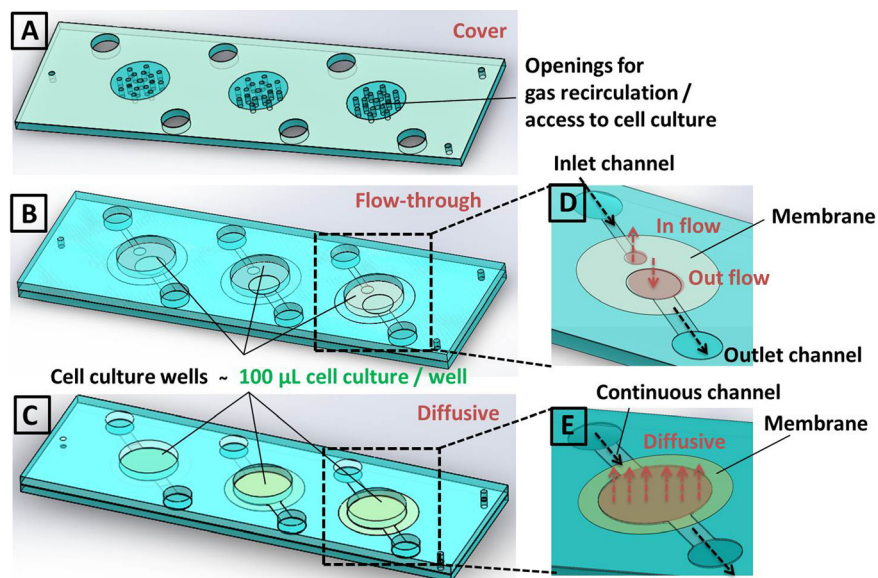

FIG. 1. Schematics of all constituent layers [(a)-(c)] and modes of operation [(d)-(e)] of the two developed fluidic design concepts: top part of the chip containing holes for access to cell culture and gas recirculation (a), bottom part of the chip containing a fluidic channel, a membrane, and a well before sealing with the top part for the flow-through (b) and diffusion-based (c) designs, operational principle shown on example of a single well for flow-through (d) and diffusion-based (e) platforms.

the configuration for the convection (Fig. 1(b)) and diffusion mode (Fig. 1(c)), respectively. The low-dead-volume polycarbonate membrane with pore sizes ranging between 0.015 μm and 0.4 μm plays two critical roles in this study: first, it serves as a cell culture support and physical barrier for suspended cells against contaminants. Second, the membrane permits continuous and controlled exposure of the cells to various concentrations of a (media diluted) chemotoxic agent which is originally introduced through a channel beneath the membrane. The gas concentrations result from the interplay between the aeration through the access holes in the lid and the gas dissolved in the supplied liquid, as, for instance, shown previously in experiments where hypoxic conditions on cells are induced.[36]

We investigated two modes of operation. The first—governed mainly by the convective mode of operation (Figures 1(b) and 1(d))—is designed for rapid exposure of the cells to the dissolved chemical agents. In this case, the flow (with a defined concentration of chemotoxic agent in media) is forced from dead-ended polymer channel through the membrane into the suspended cell culture. Provided there is sufficient resistance at the aeration holes, the media will traverse the membrane towards the outlet channel. The exposure dose of a chemical agent depends on the flow rate and the diameter of both areas of the membrane that are subjected to cross-membranous flow when all other design parameters and membrane properties are kept constant.

The second mode (Figures 1(c) and 1(e)) is designed for long-term exposure by gradual diffusion of a chemotoxic agent through the porous membrane. In this case, the media with chemotoxic agent is supplied via the underlying channel and only allowed to diffuse through the pores of membrane towards the cell culture. The rate of exposure to a chemical agent depends on the flow rate and height of the out-flow channel when all other design parameters and membrane properties are kept constant.

The limiting fluidic resistances, design considerations, and relevant application in the case of both fluidic designs are discussed in more detail in the CFD modelling section in Sec. IV.

III. MATERIALS AND METHODS

A. CFD modelling

The CFD simulation was performed using the COMSOL MULTIPHYSICS 4.2a (COMSOL Group, Sweden). The following modules were used: laminar flow in transient mode, free and porous media flow, and the transport of diluted species in convection and diffusion modes. The first and second modules were used to define the flow parameters and the latter to assess the distribution of a drug within the culture well over time. In either mode, i.e., flow-through and diffusion, the transient flow profile was first calculated. After steady-state was established, a concentration step at the inlet was initiated and the advancement of the concentration profile in time inside a culture well was monitored. The dimensions and modelling parameters are summarized in Figure 5 and Table I of Appendix A. The values for permeability of the membrane were taken from the WHATMAN® website.[37]

B. Fabrication of the prototype

The prototypes were designed using AutoCAD 2012 and Solid Works 2011. Polymer rapid prototyping techniques were applied for reproducible integration of the membrane inserts into 3D PMMA platforms. The materials used for manufacturing of microfluidic prototypes were 1.5-mm thick PMMA (Radionics, Ireland) and 175-μm PMMA sheets (Goodfellow, UK), and 86-μm thick pressure sensitive adhesive layers (PSA, Adhesive Research, Ireland). The 175-μm and 1.5-mm thick PMMA sheets serve as "spacers" to increase the height of the fluidic channels and cell culture reservoirs, respectively, and to define the desired fluidic shape. Additionally, the 1.5-mm thick rigid PMMA sheets are a convenient substrate for the assembly of the thin and flexible membranes. We chose Cyclopore and Nucleopore WHATMAN (GE Healthcare, UK) membranes with pore sizes of 0.1 μm, and the majority of the cell culture experiments presented further was based on this membrane type. However, in the fluidic tests, we have adopted other porosities as well: 15 nm, 0.2 and 0.4 μm.

All layers shown in Figure 2(a) were machined individually. The 1.5-mm thick PMMA sheets were cut by a CO_2 laser ablation system (Zing 16 Laser, Epilog, USA) in the shape of a base layer to which all the following layers are aligned using alignment holes and pins, cell culture chambers for subsequent fixing of the membranes, and a cover layer. The PSA, 175-μm PMMA, and PCTEMs were cut by a standard knife plotter (ROBO Pro cutter/plotter, Graphtec, USA) featuring all interconnecting fluidic structures, the fluidic channels, and the required cross section (8 to 10 mm) of the cell culture chamber, respectively.

The layers constituting the prototype can be broken down into three functional areas (Figure 2(a)): (i) fluidic layer with a channel and a layer defining the flux area through the membrane for controlled transport of nutrients; (ii) culture wells, i.e., reservoirs for seeding the cells on the membrane; (iii) inlet/outlet area allowing access to cell culture samples as well as recirculation of gas through the chambers.

Prior to assembly, the PMMA parts were cleaned using 2% Micro 90 solution (Sigma-Aldrich) and blow-dried with a nitrogen gun. In order to ensure sterility of the cell assay chip, the PCTEMs were autoclaved at 120 °C for 20 min and subsequently inspected by High-Resolution Scanning Electron Microscopy (HRSEM) to exclude negative influence of autoclaving conditions and UV treatment and to ensure structural integrity after the assembly (Figures 2(d) and 2(e)).

The 17 aeration holes of 0.7 mm in diameter are evenly distributed around the cell culture well of the top assembly layer to allow for sufficient gas exchange and access to cell culture at all time.

To create the final device, all layers were stacked and aligned using a custom-made assembly jig shown in Figure 2(b) under sterile conditions using UV light. The layers are then irreversibly bonded by means of the PSA at room temperature (shown in Figure 2(b) for the case of devices featuring three wells). An alternative approach for assembly involved micro-milling
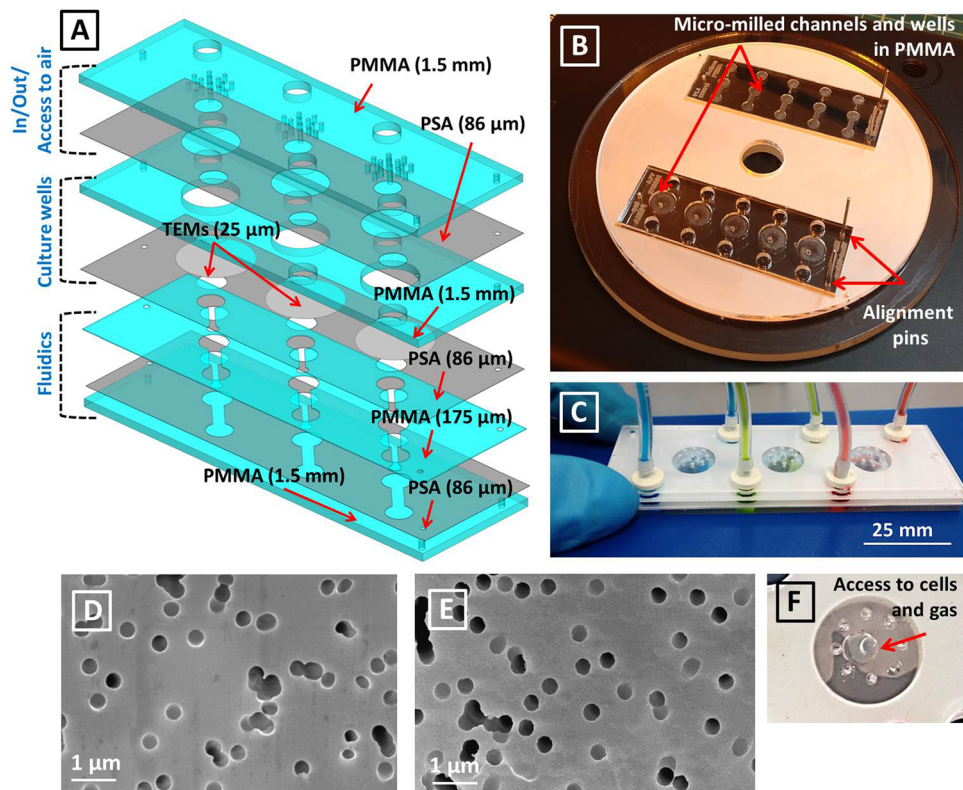

FIG. 2. Break-out of all functional layers (a); a photograph of the assembly process and an alignment jig (b); a photograph of an assembled device during the fluidic test (c); HRSEM image of the polycarbonate membranes before (d) and after (e) autoclaving and UV treatment; a photograph of a culture well loaded with cells after 24 h incubation at 37 °C and 5% CO_2 atmosphere (F).

the channels in the thick PMMA sheets similar to those shown on the device in Figure 2(b) in order to reduce the number of layers. The assembled platform (Figure 2(c)) has the convenient format of a microscopy slide (25 mm × 75 mm) that facilitates analysis of cultivated cells by standard microscopy methods.

The devices were leak-tested using the computer controlled base module and the low pressure pumping units from neMESYS (Cetoni, Germany), food colour dyes diluted in water, bondable 400 Series Barb fluidic connectors (Value plastics, Inc.), and 1.5-mm diameter Tygon tubing (Saint-Gobain Performance Plastics, France) for the flow rates ranging from 5 to 500 μl min^{-1}.

C. Trypan blue cell viability assay

The HL60 (Human myeloid leukemia) suspension cells were grown in RPMI-1640 medium with 10% FBS, 2 mM L-glutamine, and 1% penicillin-streptomycin. Following sub-culture, cells were allowed to proliferate in suspension for 48 h prior to on-chip seeding at 37 °C and 5% CO_2. When the cells reached a density of ca. 7.5×10^6 cells per ml, they were removed from culture flasks and transferred to the experimental chip.

The cells were seeded via aeration holes in the top layer and incubated on-a-chip, and a second culture was also seeded to a sterile 96-well microtiter plate for 24 h and 48 h. To verify that the PCTEMs themselves do not influence the viability of cells or the efficacy of the MMC, cells on the microtiter plate were cultivated in the presence and absence of a PCTEM at the following concentrations of MMC in media: 0, 3, 5, 10, 25, and 50 μM. The wells without the PCTEM and those without MMC were used as negative controls for examining the potential influence of the membrane material and the media on cell viability following MMC exposure, respectively. The cell viability results obtained from the microtiter plate were used as a standard calibration curve and for further comparison of assay results obtained from the chip.

For the on-chip experiment, the cells were perfused with culture media containing appropriate concentrations of MMC for 5 min and 30 min in the flow-through and diffusion-based platforms, respectively, and then transferred to a standard cell culture CO_2 incubator for 24/48 h at 37 °C and 5% CO_2. Following incubation, the cells were removed from the chip and a Trypan Blue dye exclusion viability assay was applied to the cells. A 50-μl aliquot of the removed cells was added to a tube containing 50 μl of Trypan Blue (Sigma Aldrich, MO, USA) and mixed briefly by pipetting up and down twice. An 8-μl volume of this mixture was then placed in a Bright-Line Hemocytometer (Sigma Aldrich, MO, USA) and inspected with an Olympus IX71 inverted microscope in bright-field mode (Olympus, Tokyo, JP). Viable cells were displaying as white or pink, while non-viable cells were appeared as dark or deep blue. Cell viability was reported as the percentage of viable vs the total cells count. All experiments were repeated at least 5-fold.

IV. RESULTS AND DISCUSSION

A. Operation of platforms and design considerations

Two fluidic concepts—the flow-through platform (Figures 1(b) and 1(d)) and diffusion-based platform (Figures 1(c) and 1(e))—were implemented, and the corresponding cross-sectional views with equivalent fluid resistance schemes are shown in Figures 3(a) and 3(b) (the limiting fluidic resistances in each scheme are highlighted in blue). In the sections below, the fluidic design, specific conditions imposed on cultured cells, time scale on which exposure to a chemotoxic agent is typically achieved, and potential application are discussed for each platform. In terms of the application, the cells can be subjected to either rapid or slow alternations of chemical exposures when using the two platforms.

1. Flow-through mode

The flow-through platform enables combined transport of a chemical agent by both diffusion and convection, the latter of them being dominant. The pressure drop in this system is a
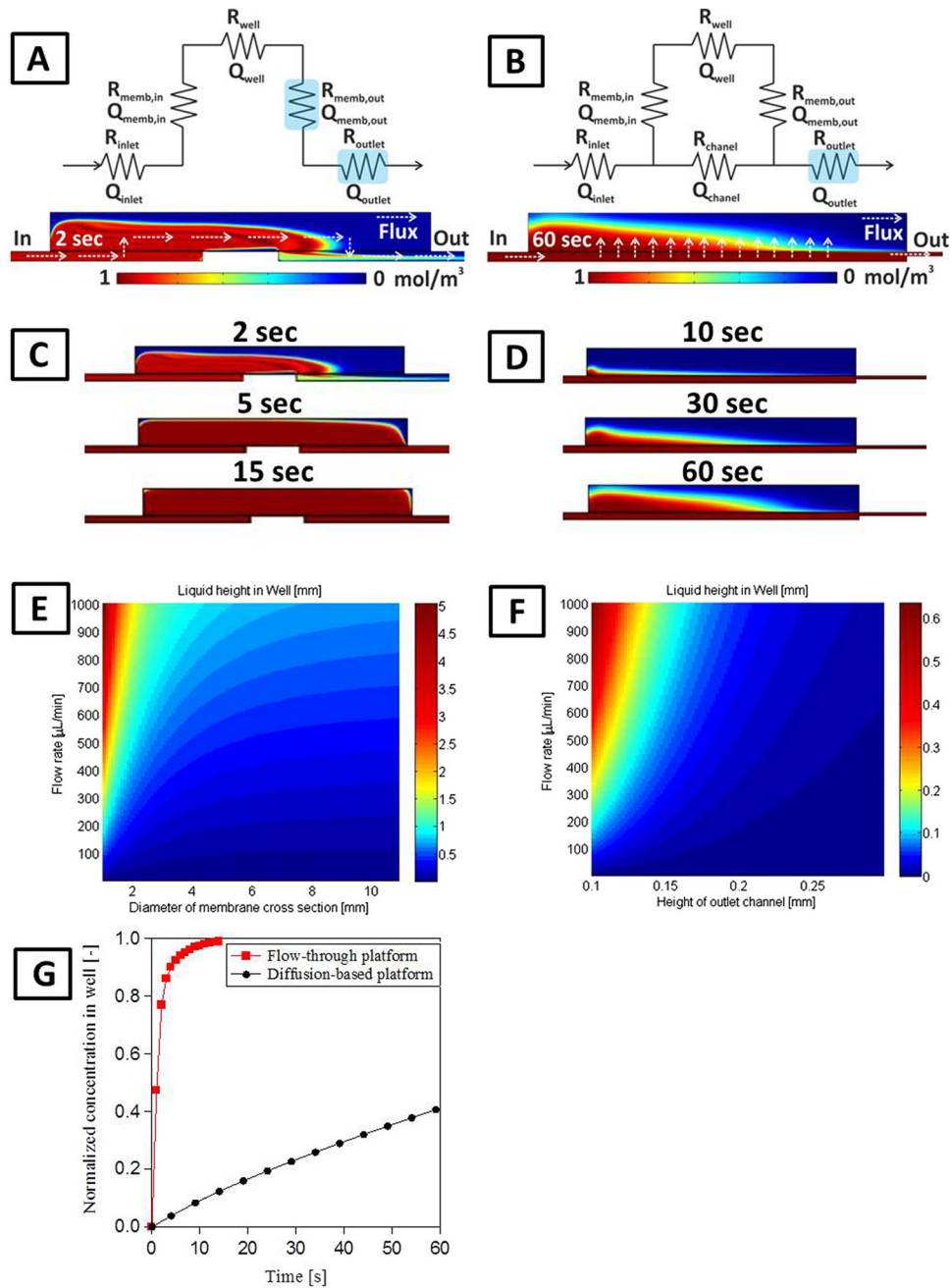
FIG. 3. Operational principle and the fluid resistance schemes (the limiting fluidic resistances are highlighted in blue) for flow-through platform (a) and diffusion-based platform (b); the development of concentration profile inside the wells with time for the flow through (c) and diffusion-based (d) platforms; the dependence of a liquid level inside a culture well on the flow rate and the characteristic dimensions of the fluidic structure or the flow through (e) and diffusive (f) platforms (diameter of the membrane cross section and height of the outlet channel for the flow through and diffusive platforms, respectively) during the device operation, the dependence of normalized concentration profile inside a culture well on time of both platforms (G).

function of the fluidic resistances of the out-flow channel and the cross-membrane out-flow—R_{outlet} and $R_{memb,out}$ (highlighted in blue in Figure 3(a)), and the flow rate at which a diluted chemical agent is supplied. Careful considerations of the above mentioned parameters will allow a sufficiently high hydrostatic pressure and the desired liquid volume of cell medium inside the well, as well as fine control over the rate of exposure to a delivered chemical agent

and gas exchange. The kinetics of mass transfer within this system occur on the scale of seconds and the uniform concentration of diluted species inside the culture well can also be achieved within seconds (Figures 3(c) and 3(g)). The CFD simulations in Figure 3(c) show that the uniform chemical concentration inside the well of the flow-through platform is achieved within less than 15 s.

Figures 3(e) shows the liquid level inside the well as a function of flow rate and diameter of the membrane area through which the flow is passing towards the outlet. The height of the liquid in the well is dependent on the equilibrium between the hydrostatic pressure in the well, the pressure drops across the outlet membrane, and the outflow channel (see Eqs. (B1) and (B2) of Appendix B). The liquid is supplied at a constant flow rate through the entire structure. The liquid viscosity and the permeability of the membrane are constant for a given system; therefore, the liquid level inside the well is controlled by the ratio of volumetric flow rate and cross-sectional membrane area of the outflow (see Eq. (B3)). If a low volume of culture medium and, correspondingly, a low liquid level in the well are desired, the cross-sectional area of the membrane should be increased and the flow rate reduced. As an example, for a flow rate of $500 \, \mu m \, min^{-1}$ and a desired liquid height of 1 mm, the diameter of the outlet membrane should be approximately 2 mm. If higher flow rates and a smaller cross-sectional area for the cross-membrane drug transport are to be established, liquid escape through the aeration holes has to be prevented. This can, for instance, be implemented by increasing the height of the well by hydrophobization[38] of the access holes or simply by covering the upper holes with a removable tape for the time the flow is applied.

As a result of cell respiration, carbon dioxide emerges an unavoidable by-product. It is removed by the liquid flow and via the vents in the cover (Figure 1(a)). In terms of the oxygen feed, one has the option of oxygen saturation through the vents in the cover or by the saturation of the liquid feed entering the well. The former (used in this study) ensures sufficient oxygen saturation of the entire well only if the liquid flow rate and the liquid height in the well are low. By the latter pre-saturation of the supplied media, the oxygen is supplied via the liquid flow passing the well.

We envision that the flow-through platform is well suited to applications where rapid changes of specific feed compositions or high dosing levels are required, possibly in combination with shear-stress studies on cells. These 3D assays might be biologically more relevant compared to the 2D systems introduced earlier for studying shear stresses on cells.[39] Compared to other systems demonstrated previously, e.g., based on hydrogel scaffolds[11,12] and targeting similar application, the present design ensures distribution of cells in the individual membrane-supported chambers with no risk of cross contamination during parallel and rapid exposure of cells to reagents. The reagents are fed via the channel and through the membrane where the cells are directly seeded, resulting in more homogeneous exposure to chemotoxic agents compared to the systems where reagents are fed from the side and rely on diffusive processes.[13] Also, due to the purely fluidic nature of the strategy used to introduce a given concentration of chemotoxic agent onto cells, a range of permitted liquid reagents is limited only by compatibility of the constructing materials, e.g., the electrochemically driven gradient generating systems involving a bipolar membrane[11] may require careful selection of liquid reagents as well as tedious calibration of experimental conditions.

2. Diffusion mode

In the case of diffusion platform featured in Figure 3(b), the cells are not exposed directly to the flow, and transport occurs exclusively via diffusion through the membrane. As shown by the development of a chemical concentration profile inside the well with the CFD simulations in Figures 3(d) and 3(g), the lack of the convective mass transport extends the time for reaching uniform concentrations to the minute scale, thus making the system more suitable for gradual chemical exposures. There is no shear stress induced on cells during operation.

In the fluidic resistance scheme shown in Figure 3(b), the liquid flow is split according to Eq. (B4) of Appendix B. A lower height in the channel below the membrane corresponds to

both a higher flow resistance and, hence, increased convection through the membrane. Using channel heights of 100 μm or more, the cells are not exposed directly to flow, and transport to and from the well is limited to cross-membrane diffusion.

The liquid height in the well is governed by the pressure drop through the outlet channel (see Eq. (B5)). Figure 3(e) shows the liquid level inside the well as a function of both the flow rate and the height of the outflow channel. So at a given flow rate, reducing the height of the out-flow channel increases the liquid level inside the culture well. Obviously, the increase in flow rate raises the liquid level in the well.

During the chip perfusion, drug-containing medium that did not cross the membrane is led to the waste. Therefore, for optimum usage of the drug, diffusion pathways should be minimized, e.g., by a low-thickness membrane and small height of the feed channel. A high mass transport is fostered by a steep concentration gradient across the membrane.

The height of the outlet channel can be designed based on a given flow rate and a desired liquid height inside the well as illustrated in Figure 3(f). Here, we assumed an outlet channel width of 1 mm and a length of 10 mm. The liquid height is one order of magnitude lower using the diffusion-controlled design. To increase the liquid height as an alternative to changing the channel dimensions, the flow restrictors downstream of the outlet channel can be used.

The exchange of oxygen and carbon dioxide required for cellular respiration is attained via both aeration vents in the cover and by diffusion through the membrane. The time required to establish the uniform distribution of a drug inside the well is often sufficient for the gas exchange, as the metabolism of the cell is slow compared to the diffusion of components using typical chip dimensions. This platform brings about slower changes of the concentration profile but also results in very homogeneous concentration profiles of gas compounds across the well. In our opinion, this makes the system more suitable for experiments where gradual changes of the cell environment are of interest, and hydrodynamic shear stress ought to be avoided.

In either operating mode, the system can be up scaled to multi-well compatible format without increasing the complexity of the current fabrication procedure. This would allow an automatized analysis of cellular assays on standard laboratory equipment,[40] thus making it competitive against some other recently demonstrated systems.[13]

B. Fabrication and membrane integration aspects

In Figures 2(d) and 2(e), the HRSEM images of the polycarbonate membranes are shown. The pores are quite evenly distributed and oriented vertically through the entire thickness of the membrane which (given a good seal by PSA) prevents any lateral leakage after assembly. Furthermore, straight channels ensure low diffusion lengths and higher drug gradients. The membranes have a very low internal pore volume (pore diameter 0.015 μm–0.4 μm) and therefore also a low internal dead-volume (inside the pores of membrane). The membrane porosity affects the dynamics of reagents delivery as flow resistance is alternated (increased with increase of pore size). The pore size of 0.1 μm was used in the majority of cell based experiments to prevent blocking of the pores by the migration of cells into the membrane. A number of tests were carried out to verify the influence of sterilisation procedures on membrane morphology and to ensure the pores are not blocked after high temperature and UV treatment. As follows from HRSEM analysis, the membranes did not modify their morphology. The chosen PCTEMs are hence suitable for sterilisation by means of UV-irradiation as well as temperature-assisted assembly processes. The purchased membranes exhibited extremely hydrophilic properties, with a membrane-water-air contact angle of ca. 15°.

Figure 2(c) shows the assembled device being leak tested with three colours of dyed water. Two types of assembly were tested with thick (150 μm) and thin (25 μm) membranes.

In the case of the first membrane integration approach, the PCTEMs were placed on PSA rings inside a shallow trench (ca. 0.5 mm deep) engraved in the middle PMMA layer by a laser. Up to 150 μm thick cellulose membranes sealed by this method resulted in leakage-free operation. However, the reproducibility of the procedure for placing the membranes in

this case was limited by the quality of the engraving procedure for the trench with a laser, in particular regarding the reproducibility of the trench height and the roughness of the surface. Typically, the variation in thickness of the laser-engraved structures is in the order of tens of microns.

In a second approach, suitable for thinner membranes, the 25-μm thick membranes were sealed between the PMMA layers only using an adhesive film. In this case, the laminate interface between the membrane and the PMMA substrate was characterized by an excellent adhesive bond, and no leakage was observed during the operation. In cellular experiments, only the devices with 25-μm thick membranes were used.

During the experiments with the flow-through design, it is important to apply hydrophobic coatings (similar to those discussed elsewhere[38]) to the gas openings to prevent liquid escape through the holes at higher flow rates due to capillary force as the liquid level in the well rises (Figure 2(f)).
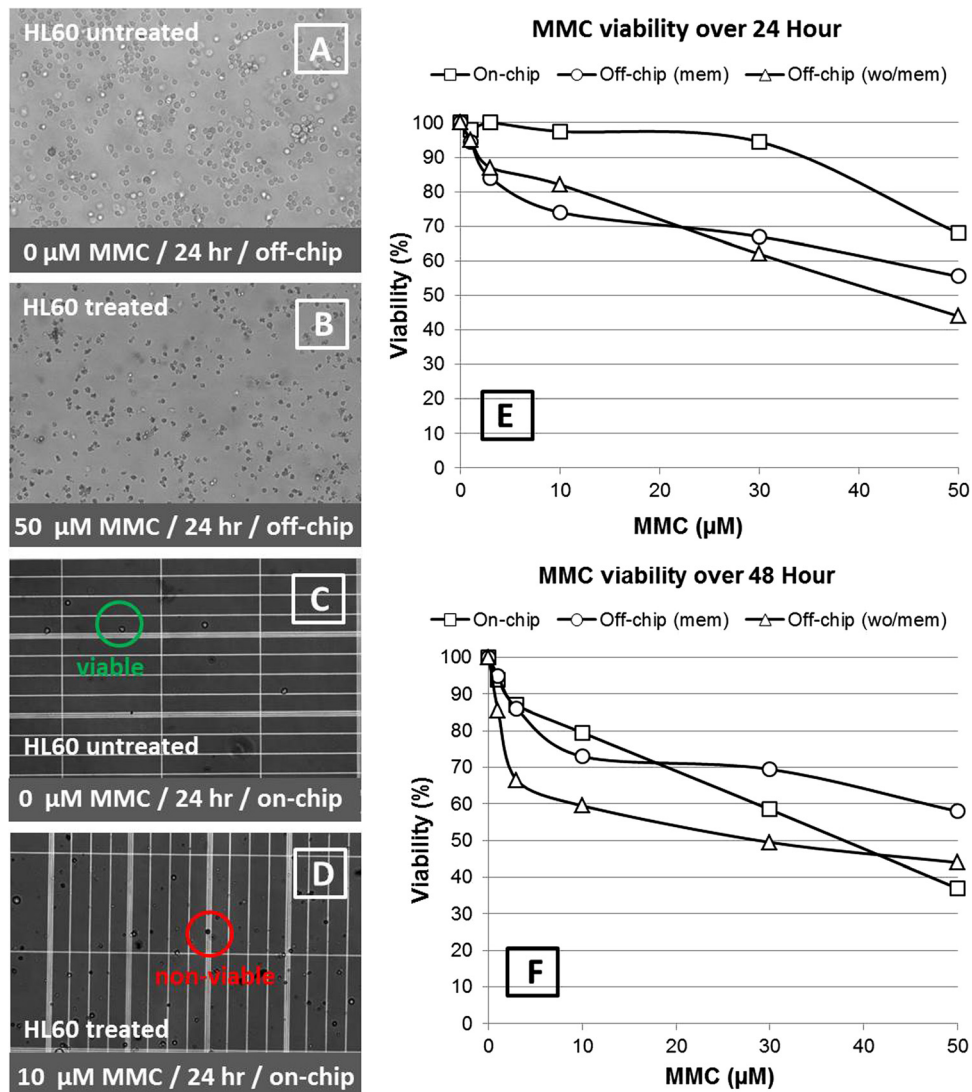

FIG. 4. Results of the viability test on HL60 following exposure to toxic MMC and incubation at 37 °C and in 5% CO_2 atmosphere for 24/48 h: optical microscopy images of cell samples 0 μM MMC (a), 50 μM MMC (b) incubated off-chip for comparison and 0 μM MMC (c), 50 μM MMC (d) taken after incubation on-a-chip; results of the viability test on HL60 with MMC for the diffusion-based platform for MMC concentrations ranging from 0 to 50 μM (e).

C. Viability assay

To demonstrate feasibility, we carried out an *in vitro* cell viability assay by controlled incubation of human HL60 cells with MMC[35] on our microfluidic platform. As described in Sec. III, the incubation was performed on-chip, while the experimental endpoint (a Trypan Blue dye exclusion viability test) was run off-chip. Figure 4 shows the images of the cells before and after the MMC treatment for samples taken from a cell assay performed in a microtiter plate run in parallel to the on-chip experiments (Figures 4(a) and 4(b)) and a chip (Figures 4(c) and 4(d)) incubated at the same conditions.

No deterioration or microbiological contamination was observed after the 48-h on-chip incubation, thus confirming that the sterilization procedure was successful and chips are suitable for long-term cell culture. The change in colour of the culture media from red to slightly yellow inside the well indicates a lowering of the pH in the media and is due to the phenol red acid/base indicator included in the media. Such a pH change is not uncommon in cell culture. However, the significantly lower volume of the culture in this case, as well as the limited capacity for gas exchange through the roof of the chip, may lead to an accelerated build-up of carbonated acids in the media. Therefore, more openings were included on the top of the chip to allow more active gas recirculation.

Figures 4(e) and 4(d) show a comparison of the viability assay performed on the diffusion-based platform with the PCTEMs of $0.1\,\mu$m porosity for the concentrations of MMC ranging from 0 to $50\,\mu$M off- and on-chip; the off-chip conditions show the viability data following culture either in the presence or absence of PCTEMs. Figure 4(e) demonstrates that higher viability was observed in the on-chip strategy for all MMC exposures at 24 h of incubation compared to a microtiter plate. The curves representing the viability after incubation with and without membranes are coherent; thus, it is evident that the presence of the membrane itself does not introduce a level of protection to cultured cells and is unlikely be a cause of the higher viability observed from the experiments on chip. Therefore, we believe this may indicate partial pore blockage by sedimenting cells resulting in delaying homogenous diffusion of the MMC. Also, the fact that the sample is manually removed from the chip in order to perform the Trypan Blue assay may introduce an error. We have, however, planned to upgrade the viability read-out of the system to use a fluorescent or luminescent viability assay (such as CellTiter-Fluor assay from promega) *in situ* on-chip. Such an upgrade will eliminate errors arising from off-chip analysis. The data obtained from the cells that were incubated for 48 h (Figure 4(f)) correspond well to the results obtained from the microtiter plate for the MMC concentrations from 0 to $10\,\mu$M, however, showing decreased viability at 30 and $50\,\mu$M MMC. Also, the results of 48 h incubation off-chip show notable difference between tests that include or exclude the presence of a PCTEM. This result was confirmed by repeating the experiment 5 times. We do not yet have a clear explanation to this effect; however, on-going experiments are investigating the effect further. No difference in performance was observed when membrane type (Cyclopore vs. Nucleopore) was changed.

V. CONCLUSIONS AND OUTLOOK

In the present paper, we describe a 3D hybrid microfluidic platform with integrated GE WHATMAN polycarbonate track-etched membranes enabling controlled cell culture and screening of chemotoxic reagents. We discussed the design and fabrication as well as convection and diffusion modes of operation for the analysis platform. In both concepts, we successfully demonstrated on-chip incubation of HL60 myeloid leukemia cells and screening of MMC exposure at concentrations between 0 and $50\,\mu$M. The results of the on-chip viability assays were well consistent with a standard curve obtained off-chip and, as an example, indicated ca. 40% survival rate at MMC concentration of $50\,\mu$M.

Forthcoming tests will expand the chip to allow multiplexing of chemotoxic exposures on cultured cells as well as rapid testing of combinations of sub-lethal drug doses of complementary agents. The objective of a future prototype is to allow clinicians to investigate the effect of

chemo-combination therapies to minimize overall agent doses for optimum cancer treatment. The conceptual simplicity, ease-of-operation, flexibility, and low-cost of the here established system make it well suited for hospital settings, doctor's offices, and remote environments where preliminary cell screening of prescribed drugs is to be performed by unskilled users.

ACKNOWLEDGMENTS

APPENDIX A: GEOMETRIES OF THE FLOW-THROUGH AND DIFFUSIVE PLATFORMS WITH THE CORRESPONDING DIMENSIONS USED IN CFD MODELLING

A 2D representation of the microfluidic platforms with the corresponding dimensions used in CFD modelling are provided below.
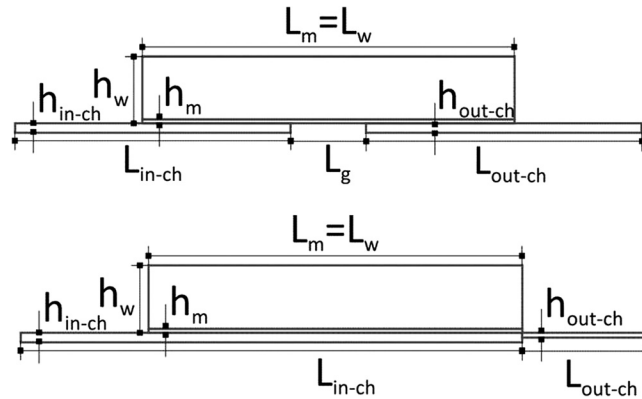

FIG. 5. Geometries of the flow-through (top) and diffusive (bottom) platforms.

TABLE I. Parameters used in the CFD modelling for the flow-through and diffusive platforms.

Parameter	Value	Description
u	$5\,\mathrm{cm\,s^{-1}}$	Flow velocity
c	$1\,\mathrm{mol\,m^{-3}}$	Normalized concentration of a drug at the inlet
T	$293.15\,\mathrm{K}$	Temperature
$h_{in\text{-}ch} = h_{out\text{-}ch}$	$250\,\mu m$	Height of the channels for the flow through design
$h_{out\text{-}ch}$[a]	$100\,\mu m$	Height of the outflow channel for the diffusive design
L_{ch}	$15\,\mathrm{mm}$	Length of the channel
L_m	$10\,\mathrm{mm}$	Total length of the membrane
L_g[a]	$2\,\mathrm{mm}$	Length of the membrane not exposed to flow
h_m	$25\,\mu m$	Thickness of the membrane
L_w	$10\,\mathrm{mm}$	Length of the culture well
h_w	$1\,\mathrm{mm}$	Height of the culture well
k	$1.23\times10^{-14}\,\mathrm{m/s}$	Permeability coefficient[37]

[a]Limiting fluidic resistance in the system.

APPENDIX B: CALCULATION OF LIQUID LEVEL INSIDE CULTURE WELL

Liquid level inside the well for the flow through platform (shown in Figures 1(b) and 1(d))

$$P_{hydrostatic} = \Delta P_{memb,out} + \Delta P_{ch,out}, \tag{B1}$$

$$\rho g H_{liquid,well} = \frac{Q_{memb,out} \cdot \mu \cdot h_{memb}}{k_{memb} \cdot A_{memb,out}} + \frac{8 \cdot \mu \cdot L_{ch,out} \cdot Q_{ch,out}}{\pi \cdot R_{ch,out}^4}, \tag{B2}$$

$$H_{liquid,well} = \frac{\frac{Q_{memb,out} \cdot \mu \cdot h_{memb}}{k_{memb} \cdot A_{memb,out}} + \frac{\varepsilon \cdot \mu \cdot L_{ch,out} \cdot Q_{ch,out}}{\pi \cdot R_{ch,out}^4}}{\rho g} \approx \frac{\frac{Q_{memb,out} \cdot \mu \cdot h_{memb}}{k_{memb} \cdot A_{memb,out}}}{\rho g}. \tag{B3}$$

Liquid level inside the well for the diffusion-based (shown in Figures 1(c) and 1(e)):

$$R_{ch} = R_{memb,in} + R_{well} + R_{memb,out} \approx R_{memb,in} + R_{memb,out}, \tag{B4}$$

$$H_{liquid,well} = \frac{\frac{\varepsilon \cdot \mu \cdot L_{ch,out} \cdot Q_{ch,out}}{\pi \cdot R_{ch,out}^4}}{\rho g}, \tag{B5}$$

where Pi is the pressure, g is the acceleration due to gravity, ρ is the density of the liquid, H_i is the height of liquid, Q_i is the volumetric flow rate, μ is the dynamic viscosity, h_i is the thickness, A_i is the cross-sectional area, L_i is the length, k_{memb} is the permeability of the membrane, and R_i is the resistance to flow.

[1] E. Sollier, C. Murray, P. Maoddi, and D. Di Carlo, Lab Chip **11**, 3752 (2011).
[2] P. Neuži, S. Giselbrecht, K. Länge, T. J. Huang, and A. Manz, Nat. Rev. Drug Discovery **11**, 620 (2012).
[3] J. Kim, D. Taylor, N. Agrawal, H. Wang, H. Kim, A. Han, K. Rege, and A. Jayaraman, Lab Chip **12**, 1813 (2012).
[4] I. K. Dimov, G. Kijanka, and J. Ducrée, in *Proceedings of the IEEE 23rd International Conference on Micro Electro Mechanical Systems (MEMS), Hong Kong* (IEEE, 2010), p. 96.
[5] I. K. Dimov, L. Basabe-Desmonts, J. L. Garcia-Cordero, B. M. Ross, Y. Park, A. J. Ricco, and L. P. Lee, Lab Chip **11**, 845 (2011).
[6] G. Kijanka, I. K. Dimov, L. P. Lee, and J. Ducrée, in *Proceedings of the 13th International Conference on Miniaturized Systems for Chemistry and Life Sciences (μTAS 2009), November 1–5, Jeju, Korea* (2009), p. 691.
[7] S. Lindström, M. Eriksson, T. Vazin, J. Sandberg, J. Lundeberg, J. Frisén, and H. Andersson-Svahn, PloS One **4**, e6997 (2009).
[8] S. Kobel, A. Valero, J. Latt, P. Renaud, and M. Lutolf, Lab Chip **10**, 857 (2010).
[9] D. Di Carlo, L. Y. Wu, and L. P. Lee, Lab Chip **6**, 1445 (2006).
[10] R. Burger, P. Reith, G. Kijanka, V. Akujobi, P. Abgrall, and J. Ducrée, Lab Chip **12**, 1289 (2012).
[11] A. Revzin, E. Maverakis, and H.-C. Chang, Biomicrofluidics **6**, 21301 (2012).
[12] A. Chen, T. Vu, G. Stybayeva, T. Pan, and A. Revzin, Biomicrofluidics **7**, 024105 (2013).
[13] E. S. Park, M. A. Difeo, J. M. Rand, and M. M. Crane, and H. Lu, Biomicrofluidics **7**, 011804 (2013).
[14] E. Vereshchagina, D. M. Glade, M. Glynn, and J. Ducrée, in *Proceedings of the 16th International Conference on Miniaturized Systems for Chemistry and Life Sciences (μTAS 2012)* (2012), p. 1855.
[15] M. Y. Rotenberg, E. Ruvinov, A. Armoza, and S. Cohen, Lab Chip **12**, 2696 (2012).
[16] J. de Jong, R. G. H. Lammertink, and M. Wessling, Lab Chip **6**, 1125 (2006).
[17] H. Hisamoto, Y. Shimizu, K. Uchiyama, M. Tokeshi, Y. Kikutani, A. Hibara, and T. Kitamori, Anal. Chem. **75**, 350 (2003).
[18] P.-C. Wang, D. L. DeVoe, and C. S. Lee, Electrophoresis **22**, 3857–3867 (2001).
[19] A. Epshteyn, S. Maher, A. J. Taylor, A. B. Holton, J. T. Borenstein, and J. D. Cuiffi, Biomicrofluidics **5**, 46501 (2011).
[20] F. Evenou, J.-M. Di Meglio, B. Ladoux, and P. Hersen, Lab Chip **12**, 1717 (2012).
[21] M. B. Esch, J. H. Sung, J. Yang, C. Yu, J. Yu, J. C. March, and M. L. Shuler, Biomed. Microdevices **14**, 895 (2012).
[22] N. Ferrell, R. R. Desai, A. J. Fleischman, S. Roy, H. D. Humes, and W. H. Fissell, Biotechnol. Bioeng. **107**, 707 (2010).
[23] I. Hutter, E. Müller, P. M. Kristiansen, S. Kresak, and L. Tiefenauer, Microfluid. Nanofluid. **14**(3–4), 421–429 (2013).
[24] M. He, J. Novak, B. A. Julian, and A. E. Herr, J. Am. Chem. Soc. **133**, 19610 (2011).
[25] D. Huh, G. A. Hamilton, and D. E. Ingber, Trends Cell Biol. **21**, 745 (2011).
[26] D. Huh, B. D. Matthews, A. Mammoto, M. Montoya-Zavala, H. Y. Hsin, and D. E. Ingber, Science (N.Y.) **328**, 1662 (2010).
[27] S. Srigunapalan, C. Lam, A. R. Wheeler, and C. Simmons, Biomicrofluidics **5**, 13409 (2011).
[28] G. Si, W. Yang, S. Bi, C. Luo, and Q. Ouyang, Lab Chip **12**, 1389 (2012).
[29] M. Adler, M. Erickstad, E. Gutierrez, and A. Groisman, Lab Chip **12**, 4835 (2012).
[30] K. B. Neeves and S. L. Diamond, Lab Chip **8**, 701 (2008).
[31] T. Masters, W. Engl, Z. L. Weng, B. Arasi, N. Gauthier, and V. Viasnoff, PloS One **7**, e44261 (2012).

[32]E. Karatay and R. G. H. Lammertink, Lab Chip **12**, 2922 (2012).
[33]D. Snakenborg, H. Klank, and J. P. Kutter, Microfluid. Nanofluid. **10**, 381 (2010).
[34]P. J. Kitson, M. H. Rosnes, V. Sans, V. Dragone, and L. Cronin, Lab Chip **12**, 3267 (2012).
[35]M. Sasaki, M. Okamura, A. Ideo, J. Shimada, F. Suzuki, M. Ishihara, H. Kikuchi, Y. Kanda, S. Kunii, and H. Sakagami, Anticancer Res. **26**, 3373 (2006).
[36]K. Funamoto, I. K. Zervantonakis, Y. Liu, C. J. Ochs, C. Kim, and R. D. Kamm, Lab Chip **12**, 4855 (2012).
[37]See www.whatman.com for structural and chemical properties of polymeric membrane inserts.
[38]M. Kitsara and J. Ducrée, J. Micromech. Microeng. **23**, 033001 (2013).
[39]L. Chau, M. Doran, and J. Cooper-White, Lab Chip **9**, 1897 (2009).
[40]E. Vereshchagina, D. Mc Glade, M. Glynn, and J. Ducrée, in Proceedings of the 17th International Conference on Solid-State Sensors, Actuators & Microsystems (Transducers 2013), Barcelona, Catalonia, Spain 16–20 June 2013.